

JAERI-M
7 8 6 2

STUDIES ON LOW-VOLTAGE X-RAY RADIOGRAPHY
FOR GRAPHITE MATERIALS

September 1978

Susumu MURAOKA and Hiroharu ITAMI

この報告書は、日本原子力研究所が JAERI-M レポートとして、不定期に刊行している研究報告書です。入手、複製などのお問い合わせは、日本原子力研究所技術情報部（茨城県那珂郡東海村）あて、お申しこしてください。

JAERI-M reports, issued irregularly, describe the results of research works carried out in JAERI. Inquiries about the availability of reports and their reproduction should be addressed to Division of Technical Information, Japan Atomic Energy Research Institute, Tokai-mura, Naka-gun, Ibaraki-ken, Japan.

Studies on Low-Voltage X-ray Radiography for Graphite
Materials

Susumu MURAOKA and Hiroharu ITAMI

Division of JMTR Project,
Oarai Research Establishment, JAERI

(Received August 18, 1978)

Low-voltage radiography has been studied to provide optimum technique for graphite less than 50 mm thick. First we determined the exposure conditions under which the most appropriate photographic density can be obtained. By parametric studies, an exposure chart was prepared. Then we studied how the environment of photographing affected the film density. Thirdly, by use of graphite materials with artificial flaws, Image Quality Indicator (I.Q.I.) sensitivity was determined. Detectability of a crack depended on an incidence angle of X-rays onto a crack. Finally, we photographed graphites having natural flaws and gained a useful information.

Keywords: Low-Voltage Radiography, Graphite, Exposure Chart,
Film Density, Image Quality Indicator Sensitivity,
Crack, Flaw, Exposure Conditions.

軟X線によるグラファイトの放射線透過試験

日本原子力研究所大洗研究所材料試験炉部

村岡 進・伊丹宏治

(1978 年8月18日 受理)

軟X線発生装置を使用して、1～50 mm 厚さのグラファイトの放射線透過試験を行った。まず、欠陥を検出するのに最適なフィルム濃度を得るための露出線図を作成するとともに、フィルムの像質におよぼす、線源 ↔ フィルム間の雰囲気、フィルムホルダー等による放射線の散乱、吸収の影響について検討を行った。次に、模擬欠陥を有するグラファイトを用い、欠陥の識別度を求めた。更に、クラックゲージを作成して、割れタイプの欠陥の検出の限界を求めると共に、自然欠陥への適用を試みた。

Contents

1. Introduction	1
2. Theory	2
3. Experimental Procedures	3
3.1 Experiment in air	4
3.2 Experiment in vacuo	5
3.3 Crack detectability test	6
4. Results and Discussion	6
4.1 Experiment in air	6
4.2 Experiment in vacuo	7
4.3 Crack detectability test	7
5. Application	8
6. Conclusions	8
Acknowledgements	9
References	9

1. Introduction

Graphite possesses good nuclear properties, high temperature properties and stability, so this material is being rapidly developed for nuclear and aerospace uses. In nuclear industries, graphite has been used as neutron reflector and core structural material in Calder Hall type power reactors and advanced gas cooled reactors. Japan Atomic Energy Research Institute has proceeded with the research and development for experimental Very High Temperature Gas-cooled Reactor (VHTR) since 1969.⁽¹⁾

In this reactor large amounts of graphite will be used as the core structural material and fuel sleeve. In fusion reactors low atomic number ceramic materials such as graphite are planned to be the first wall of plasma feasibility devices. Graphite or carbon is selected to be a promising material.⁽²⁾ The utilization of such materials demands the use of high confidence inspection techniques to ensure material integrity. For this purpose non-destructive examination plays an important role. As for non-destructive examinations applicable to graphite, there are radiographic, ultrasonic and liquid penetrant test. The latter two tests are not usable because a liquid must be used as a couplant or penetrant and the inspected surface is apt to be contaminated.

However a radiographic inspection has no such faults so that it is thought the most useful method. There are few users or manufacturer using radiographic examination in quality control and acceptance inspection in the world. We can only find a description of the process specifications in Westinghouse Electric Cooperation Astronuclear Laboratory in the U.S.A.⁽³⁾

R.W. McClung of ORNL (OakRidge National Laboratory) reported about applicability of low voltage radiography to an inspection of graphite and Beryllium materials.⁽⁴⁾ But he did not study discrimination and estimation of flaws from practical points of view. The main purpose of the present study is to provide information on the applicability and utility of radiographic examination for graphite. By use of low voltage X-ray equipment, we find the exposure conditions for best photographs and determine the visible limits of flaws with using artificial flaws. We made experiments on the effects of atmosphere and film holder on the image in detail. Furthermore, we studied the effect of an incidence angle of X-rays onto a crack. We inspected real graphite material by

use of materials having both artificial cracks and natural flaws.

2. Theory

As is well known, a radiographic method consists of transmitting a beam of X-ray or gamma-ray radiation through a test specimen and recording the transmitted radiation intensity on a medium such as film. Variation in the transmission properties of the specimen will cause variation in the recording medium. This system follows the law⁽⁵⁾

$$I = I_0 e^{-\mu T} \quad (1)$$

Equation (1) states that if a source emits the radiation of intensity I_0 , the amount of intensity remaining is I after traversing the thickness of material T with absorption coefficient μ . The μ value is derived from interaction processes by which radiation is "deflected" by the particular atom species of which the absorber is composed. These "deflection" may occur by photoelectric effect, Compton scattering, inelastic collision and pair production. In the wide range of energies used in non-destructive testing a energy function can not be simply described, and, in fact, is a discontinuous function. The μ value depends on geometry of the absorption system measured. I , the transmitted portion of I_0 , is the portion that traverses the absorber without the interactions mentioned above, and is recorded on a detection system. Any radiation other than this unaltered primary beam which reaches a film contributes to the error in accuracy of this description of the absorption process. Such contributions in practical cases come from the detector registered scattering of the primary beam.

The ability to detect a change in transmitted radiation intensity will partly depends on the change intensity will partly depends on the change in the exponential terms μ and T across the projected area of a specimen. It is evident that the larger the exponent terms, the larger the radiation attenuation and consequently the greater the change in intensity. To get useful radiography, there must be sufficient variation in the radiation absorption by the specimen for an interpretable density contrast achieved on a film or other detector. The μ value is energy dependent with generally increasing values occurring at decreasing energy levels. Therefore it is necessary to use low-energy radiography in case

use of materials having both artificial cracks and natural flaws.

2. Theory

As is well known, a radiographic method consists of transmitting a beam of X-ray or gamma-ray radiation through a test specimen and recording the transmitted radiation intensity on a medium such as film. Variation in the transmission properties of the specimen will cause variation in the recording medium. This system follows the law⁽⁵⁾

$$I = I_0 e^{-\mu T} \quad (1)$$

Equation (1) states that if a source emits the radiation of intensity I_0 , the amount of intensity remaining is I after traversing the thickness of material T with absorption coefficient μ . The μ value is derived from interaction processes by which radiation is "deflected" by the particular atom species of which the absorber is composed. These "deflection" may occur by photoelectric effect, Compton scattering, inelastic collision and pair production. In the wide range of energies used in non-destructive testing a energy function can not be simply described, and, in fact, is a discontinuous function. The μ value depends on geometry of the absorption system measured. I , the transmitted portion of I_0 , is the portion that traverses the absorber without the interactions mentioned above, and is recorded on a detection system. Any radiation other than this unaltered primary beam which reaches a film contributes to the error in accuracy of this description of the absorption process. Such contributions in practical cases come from the detector registered scattering of the primary beam.

The ability to detect a change in transmitted radiation intensity will partly depends on the change intensity will partly depends on the change in the exponential terms μ and T across the projected area of a specimen. It is evident that the larger the exponent terms, the larger the radiation attenuation and consequently the greater the change in intensity. To get useful radiography, there must be sufficient variation in the radiation absorption by the specimen for an interpretable density contrast achieved on a film or other detector. The μ value is energy dependent with generally increasing values occurring at decreasing energy levels. Therefore it is necessary to use low-energy radiography in case

of thin section and light materials. This provides a large enough absorption coefficient to permit the detection of a minute thickness change associated with discontinuity of an interest. The μ values for various atoms are given in Table 1. When radiographic test is carried out using photographic method, the relation between ΔD and ΔT , difference of film contrast and material's thickness respectively, is shown as follows

$$\Delta D = -0.4343\gamma\mu\Delta T \quad (2)$$

where γ : film contrast,

μ : absorption coefficient.

We must consider the scattering of X-rays which comes from not only from the back side of a film but also from the interior of a specimen. In this case, equation (2) is represented as

$$\Delta D = -0.4343\gamma\mu\frac{E}{E+S}\Delta T \quad (3)$$

where E : dose by direct X-rays,

S : dose by scattered X-rays.

As described above, it depends on two factors, sharpness and contrast of the film, whether the flaw can be detected or not. Sharpness depends on size of the source, film-source distance, specimen-film distance and the kinds of film and intensifying screen. Film contrast depends on the applied voltage, X-ray quality, developing conditions and the kinds of film and intensifying screen. Naturally, the better the sharpness and contrast of the film are, the better the image quality is. By photographing the "Image Quality Indicator" (I.Q.I.) together with the specimen at the same time, we measure the image quality. There are two types of I.Q.I., a wire type and a hole type. Usually the I.Q.I. sensitivity is different from the shape of I.Q.I., so that it shows not real flaw visibility but merely a criterion. Generally, there exists the threshold area of the image where the contrast depends on the I.Q.I. sensitivity.

3. Experimental Procedures

Throughout the experiments, we used a commercial low energy X-ray

of thin section and light materials. This provides a large enough absorption coefficient to permit the detection of a minute thickness change associated with discontinuity of an interest. The μ values for various atoms are given in Table 1. When radiographic test is carried out using photographic method, the relation between ΔD and ΔT , difference of film contrast and material's thickness respectively, is shown as follows

$$\Delta D = -0.4343\gamma\mu\Delta T \quad (2)$$

where γ : film contrast,

μ : absorption coefficient.

We must consider the scattering of X-rays which comes from not only from the back side of a film but also from the interior of a specimen. In this case, equation (2) is represented as

$$\Delta D = -0.4343\gamma\mu\frac{E}{E+S}\Delta T \quad (3)$$

where E : dose by direct X-rays,

S : dose by scattered X-rays.

As described above, it depends on two factors, sharpness and contrast of the film, whether the flaw can be detected or not. Sharpness depends on size of the source, film-source distance, specimen-film distance and the kinds of film and intensifying screen. Film contrast depends on the applied voltage, X-ray quality, developing conditions and the kinds of film and intensifying screen. Naturally, the better the sharpness and contrast of the film are, the better the image quality is. By photographing the "Image Quality Indicator" (I.Q.I.) together with the specimen at the same time, we measure the image quality. There are two types of I.Q.I., a wire type and a hole type. Usually the I.Q.I. sensitivity is different from the shape of I.Q.I., so that it shows not real flaw visibility but merely a criterion. Generally, there exists the threshold area of the image where the contrast depends on the I.Q.I. sensitivity.

3. Experimental Procedures

Throughout the experiments, we used a commercial low energy X-ray

radiographic instrument, Radio Flex 100 GS. In experiments of §3.1 and §3.2, the specimen was a SEG-6H type high purity reactor grade graphite purchased from Nippon Carbon CO. LTD.. The properties are shown in Table 2. With this graphite a step wedge meter, shown in Fig. 1, and a ditch type I.Q.I., Fig. 2, were fabricated. Two kinds of film were used, Sakura RR and Eastman M (equivalent to Sakura R). Intensifying papers were not used throughout the experiments. The cross section of ditch was shaped nearly oval, with long radius 20 mm and short radius 10 mm, and the depth varying with geometric ratio. This I.Q.I. was also used as an example of artificial flaw.

The low energy X-rays are suitable to inspect low absorption materials such as graphite and aluminum and not for steel. When low energy X-rays are used, it is necessary to examine the effect of air between radiation source and film and of absorption or scattering by the film holder which can be neglected under high energy photography. By using a vacuum chamber shown in Fig. 3, we carried out the experiment in a vacuum or not using film holder and examined the influences of air and film holder on the I.Q.I. sensitivity. Fuji Hi-Rendol was used as developer and Fuji Hi-Renfix as fixer, Developing temperature and time were kept 20°C and 5 minutes constantly. The film was observed in a dark room with a Seiko film viewer. A manual densitometer, Macbeth TD-100 A type, was used to determine the photographic film density at each reduced thickness and its minimum graduation was 0.2.

3.1 Experiment in air

This experiment was carried out not using vacuum chamber. A film holder is made of paper the same as that used in the experiment §3.2. First we attempted to obtain exposure charts. For parameters of determining the exposure conditions, there are sensitivity of radiographic film, specimen thickness, voltage and current of irradiation X-rays, irradiation time, radiation source-film distance and film density. We fixed the radiation source-film distance 60 cm and plotted the exposure parameters to obtain the exposure conditions that made the film density "2". For the relation between film contrast and density, graphite specimens of thicknesses 5, 10 and 20 mm with 1-5 mm thick contrastmeter were photographed at the same time. Measuring was carried out according to JIS Z 3105⁽⁶⁾: Method of Radiography and Classification for Aluminum

Welds. The I.Q.I. sensitivity was determined for the film photographed under best conditions. The I.Q.I. sensitivity was obtained from the following formula

$$\text{I.Q.I. sensitivity} = \frac{\text{Minimum depth of I.Q.I. found in test part (mm)}}{\text{Thickness of test part (mm)}} \times 100$$

It is impossible to compare the I.Q.I. with the size of actually visible flaws. In this experiment, we tried to obtain a criterion of size limitation of conceivable flaws. The used I.Q.I., shown in Fig. 2, was so wide that the width of the image did not affect visible density difference.

Minimum machinable depth of the artificial flaws in I.Q.I. was 0.1 mm. By this method it was so difficult to make the standard flaw thinner than 0.1 mm on 1-5 mm thickness graphite material that it was impossible to discuss the I.Q.I. sensitivity on thin materials. Furthermore we made wire type I.Q.I. i.e. 0.05 mm diameter whisker. The results of experiment with this I.Q.I. show difficulty of detecting because of its size effect due to X-ray scattering or harration.

3.2 Experiment in vacuo

By use of a vacuum chamber we tried to clarify the effects of scattering and absorbing by the environment such as air, vacuum chamber etc. The experiment was carried out by four kinds of combination as below

	atmospherent	film holder
(1)	vacuo ^(*)	not used
(2)	vacuo	used
(3)	air	not used
(4)	air	used

Note (*) about 10 - 20 mmHg

In this experiment specimens having various thicknesses were photographed. Effects of vacuum chamber, air and film holder were estimated respectively by measuring the film densities. The conditions of experiment were fixed as same as possible. The conditions and factors were all same as in experiment in air. Sakura RR film was used throughout and an intensifying paper was not used. A radiation source-film distance was fixed at 60 cm.

The film holder was paper used as a wrapper of Kodak paper film. The color outside the holder was red and inside black. Its thickness was 0.15 mm. In order to indentify the conditions of photography, a film was used by inserting the half part into the film holder. Experiments (1) and (2) were carried out at the same time and (3) and (4) similarly. In series of these experiments developing treatment was carried out at the same time to reduce the effect of conditions.

3.3 Crack detectability test

In §3.1 we treated flaws somewhat round like prosity or disk type defect. In order to examine detectability of cracks and lamminar type defects that have marked influence on reduction of material strength, the experiment was carried out by use of graphite with an artificial crack. Slit or crack detection is sensible to such factors as image contrast, slit size, unsharpness and inclination of the slit plane in beam direction. It is especially important to pay close attention to the exisistence of these types of defect in radiography. We also compared between three kinds of graphite specimen, SM1-24, SE2-24 and SMG. Properties of these graphite are shown in Table 2. An artificial crack (defect) was formed by putting various thickness guage between two graphite blocks as shown in Fig. 4. The sizes of the used thickness guages were 0.04, 0.10, 0.15 and 0.20 mm respectively.

The test was carried out by selecting an inclined angle and graphite material thickness as parameters. All the tests were carried out in air, so that the film was photographed covered with paper holder. The arrangement of X-ray equipment is shown in Fig. 5 and the conditions of experiments in Table 3.

4. Results and Discussion

4.1 Experiment in air

In Figs. 6 and 7 exposure charts are shown for two types of film Sakura RR and Eastman M. Exposure charts are drawn by selecting the thickness of specimens as a parameter. In Fig. 8 is shown the relation of film contrast and material thickness, 5, 10 and 20 mm. In case of 5 and 10 mm thick materials, Eastman M type film was superior in contrast to Sakura RR type film. There was no difference between two

The film holder was paper used as a wrapper of Kodak paper film. The color outside the holder was red and inside black. Its thickness was 0.15 mm. In order to indentify the conditions of photography, a film was used by inserting the half part into the film holder. Experiments (1) and (2) were carried out at the same time and (3) and (4) similarly. In series of these experiments developing treatment was carried out at the same time to reduce the effect of conditions.

3.3 Crack detectability test

In §3.1 we treated flaws somewhat round like prosity or disk type defect. In order to examine detectability of cracks and lamminar type defects that have marked influence on reduction of material strength, the experiment was carried out by use of graphite with an artificial crack. Slit or crack detection is sensible to such factors as image contrast, slit size, unsharpness and inclination of the slit plane in beam direction. It is especially important to pay close attention to the exisistence of these types of defect in radiography. We also compared between three kinds of graphite specimen, SM1-24, SE2-24 and SMG. Properties of these graphite are shown in Table 2. An artificial crack (defect) was formed by putting various thickness guage between two graphite blocks as shown in Fig. 4. The sizes of the used thickness guages were 0.04, 0.10, 0.15 and 0.20 mm respectively.

The test was carried out by selecting an inclined angle and graphite material thickness as parameters. All the tests were carried out in air, so that the film was photographed covered with paper holder. The arrangement of X-ray equipment is shown in Fig. 5 and the conditions of experiments in Table 3.

4. Results and Discussion

4.1 Experiment in air

In Figs. 6 and 7 exposure charts are shown for two types of film Sakura RR and Eastman M. Exposure charts are drawn by selecting the thickness of specimens as a parameter. In Fig. 8 is shown the relation of film contrast and material thickness, 5, 10 and 20 mm. In case of 5 and 10 mm thick materials, Eastman M type film was superior in contrast to Sakura RR type film. There was no difference between two

kinds of film in 20 mm thick graphite material. Where the density exceeds 2.0, the contrast curves become saturated. The film density at least 2.0 is required. In observation of the film the density between 2.0 and 3.0 is necessary. When the film viewer is enough light we can observe the film even if the density is 3.5. Table 4 shows a I.Q.I. sensitivity of 20-40 mm thick graphite. Reasonably the I.Q.I. sensitivity depends on vision power of the inspectors so there exists individual difference. The I.Q.I. sensitivity of 0.40 % is much excellent. This is because in JIS the I.Q.I. sensitivity for steel or aluminum below 1.5% at a special class is required.

4.2 Experiment in vacuo

(1) Effect of the atmosphere

In Fig. 9 the relation between the energy and film density is compared between respective thickness graphite specimen. From this figure the effect of atmosphere is large where X-ray energy is below 30 kvp and density is over 1.5. Where the energy is above 40 kvp and the density is less than 1.5, the effect of atmosphere is negligible. Fig. 9 shows that the absorption of radiated X-rays by air is large and it reaches to 50-60 % in case of 15 kvp of X-ray energy. At 40 kvp or more it can be neglected.

(2) Effect of the film holder

Effect of the film holder was observed and the results are shown in Fig. 10. As seen in the figure when the density is less than 2.0 the effect is very little. An interesting phenomenon is observable. Near 35-40 kvp of X-ray energy and density 2.0, the effect is reversed from $(V_b) > (V_p)$ to $(V_p) > (V_b)$. Here (V_b) represents the film density photographed without film holder and (V_p) represents that in paper holder in vacuum atmosphere. The effects of various environments are compared in Figs. 11, 12 and Table 6.

4.3 Crack detectability test

In observing the film, the difference between individual observers is not avoidable and it is difficult to get meaningful quantitative results. We chose the limits where flaws can be detected clearly by anyone who are not used to observe film. In Figs. 13-16 the detectability

lity limits are shown in slit width. From these figures, it is evident that the crack detectability depends on width of the slit and the beam-specimen inclination angle. By inclining the X-ray beam 9° or less a crack 0.04 mm wide was just detectable and by 18° a crack 0.2 mm wide was detectable.

As shown in Fig. 16, for specimens of 10 mm thick, a crack with depth 10 mm will not be detected radiographically where the width is about 0.04 mm or less.

5. Application

There are many kinds of nuclear graphite, which are different in composition, fabrication method, grain size, density etc. Absorption coefficients for X-rays changes between the kinds of material. We compared three kinds of graphite SM1-24, SE2-24 and SMG. The size of graphite blocks was 50 mm square and the thicknesses were 10, 20, 30 and 40 mm. These specimens were photographed under the same conditions as in Fig. 7. The film density is lower in the order of their density shown in Table 6.

In case of SE2-24 micro cracks were found out as in Fig. 17. In the experiment, the cracks parallel to the X-ray beam direction could be observed but those perpendicular could not be observed.

By use of a fatigue test facility a artificial crack was made in SM1-24 specimen (10 mm thick) as shown in Fig. 18. This crack was resembled a natural crack in shape and could be detected if it was parallel to the beam direction but not in other directions. Fig. 19 is the X-ray radiography of the artificial crack. We made inspection actually on graphite blocks. Graphite materials (SM1-24), 50 mm thick, was radiographed by means of the exposure chart in Fig. 7. Fig. 20 is a external view of the cracked graphite. The crack parallel to the surface could not be detected. On the other hand, the crack perpendicular to the surface could be detected clearly as in Fig. 21.

6. Conclusions

- (1) Low voltage radiographic inspection method is useful for graphite materials thinner than about 50 mm thick. We drew up exposure charts by low energy X-ray equipment. Especially for the thin

lity limits are shown in slit width. From these figures, it is evident that the crack detectability depends on width of the slit and the beam-specimen inclination angle. By inclining the X-ray beam 9° or less a crack 0.04 mm wide was just detectable and by 18° a crack 0.2 mm wide was detectable.

As shown in Fig. 16, for specimens of 10 mm thick, a crack with depth 10 mm will not be detected radiographically where the width is about 0.04 mm or less.

5. Application

There are many kinds of nuclear graphite, which are different in composition, fabrication method, grain size, density etc. Absorption coefficients for X-rays changes between the kinds of material. We compared three kinds of graphite SM1-24, SE2-24 and SMG. The size of graphite blocks was 50 mm square and the thicknesses were 10, 20, 30 and 40 mm. These specimens were photographed under the same conditions as in Fig. 7. The film density is lower in the order of their density shown in Table 6.

In case of SE2-24 micro cracks were found out as in Fig. 17. In the experiment, the cracks parallel to the X-ray beam direction could be observed but those perpendicular could not be observed.

By use of a fatigue test facility a artificial crack was made in SM1-24 specimen (10 mm thick) as shown in Fig. 18. This crack was resembled a natural crack in shape and could be detected if it was parallel to the beam direction but not in other directions. Fig. 19 is the X-ray radiography of the artificial crack. We made inspection actually on graphite blocks. Graphite materials (SM1-24), 50 mm thick, was radiographed by means of the exposure chart in Fig. 7. Fig. 20 is a external view of the cracked graphite. The crack parallel to the surface could not be detected. On the other hand, the crack perpendicular to the surface could be detected clearly as in Fig. 21.

6. Conclusions

- (1) Low voltage radiographic inspection method is useful for graphite materials thinner than about 50 mm thick. We drew up exposure charts by low energy X-ray equipment. Especially for the thin

lity limits are shown in slit width. From these figures, it is evident that the crack detectability depends on width of the slit and the beam-specimen inclination angle. By inclining the X-ray beam 9° or less a crack 0.04 mm wide was just detectable and by 18° a crack 0.2 mm wide was detectable.

As shown in Fig. 16, for specimens of 10 mm thick, a crack with depth 10 mm will not be detected radiographically where the width is about 0.04 mm or less.

5. Application

There are many kinds of nuclear graphite, which are different in composition, fabrication method, grain size, density etc. Absorption coefficients for X-rays changes between the kinds of material. We compared three kinds of graphite SM1-24, SE2-24 and SMG. The size of graphite blocks was 50 mm square and the thicknesses were 10, 20, 30 and 40 mm. These specimens were photographed under the same conditions as in Fig. 7. The film density is lower in the order of their density shown in Table 6.

In case of SE2-24 micro cracks were found out as in Fig. 17. In the experiment, the cracks parallel to the X-ray beam direction could be observed but those perpendicular could not be observed.

By use of a fatigue test facility a artificial crack was made in SM1-24 specimen (10 mm thick) as shown in Fig. 18. This crack was resembled a natural crack in shape and could be detected if it was parallel to the beam direction but not in other directions. Fig. 19 is the X-ray radiography of the artificial crack. We made inspection actually on graphite blocks. Graphite materials (SM1-24), 50 mm thick, was radiographed by means of the exposure chart in Fig. 7. Fig. 20 is a external view of the cracked graphite. The crack parallel to the surface could not be detected. On the other hand, the crack perpendicular to the surface could be detected clearly as in Fig. 21.

6. Conclusions

- (1) Low voltage radiographic inspection method is useful for graphite materials thinner than about 50 mm thick. We drew up exposure charts by low energy X-ray equipment. Especially for the thin

material less than 5 mm thick, control of atmosphere and bare film exposure techniques are useful.

- (2) The absorption of radiated X-rays by air is large and it reaches to 50-60 % in case of 15 kvp of X-ray energy. At 40 kvp or more it can be neglected.
- (3) The difference in radiographic quality between two types of film, Sakura RR and Eastman M, were compared in the sensitivity and contrast. The sensitivity of Sakura RR is about 10 times higher than that of Eastman M. Image contrast depends on the thickness of material. In case of 5 and 10 mm thick material Eastman M is superior to Sakura RR, but at 20 mm there is no difference between them.
- (4) The I.Q.I. sensitivity obtained for 20 mm thick material is 0.5 %. This value is excellent as the radiographic film.
- (5) Within the scope of study the detectability of cracks is dependent on the incidence angle of X-rays to the cracks. It is desirably less than 9°.

Acknowledgement

The authors wish to thank Drs. S. Nomura, Y. Sasaki and T. Oku for their informative advice.

Thanks are also due to Mr. Fujisaki and the member of the Graphite Research Lab. for many experimental helps.

References

- 1) Shimokawa J. et al. : JAERI-M 6141, "Fundamental Conceptual Design of the Experimental Multi-Purpose High-Temperature Gas-Cooled Reactor" (1975)
- 2) Gomay Y., Nomura S., Fukuda K., Muraoka S. and Nakamura H. : JAERI-M 6432, "An Estimate of Low-Z Materials for the First Wall of JT-60" (1974)
- 3) Westinghouse Electric Corporation, Astro Nuclear Laboratory : WANL-TME-391, "Requirements for Unloaded Graphite Core Elements for WANL Destruction Core Test" (1973)
- 4) McClung R.W. : ORNL-3252, "Techniques for Low-Voltage Radiography" (1962)

material less than 5 mm thick, control of atmosphere and bare film exposure techniques are useful.

- (2) The absorption of radiated X-rays by air is large and it reaches to 50-60 % in case of 15 kvp of X-ray energy. At 40 kvp or more it can be neglected.
- (3) The difference in radiographic quality between two types of film, Sakura RR and Eastman M, were compared in the sensitivity and contrast. The sensitivity of Sakura RR is about 10 times higher than that of Eastman M. Image contrast depends on the thickness of material. In case of 5 and 10 mm thick material Eastman M is superior to Sakura RR, but at 20 mm there is no difference between them.
- (4) The I.Q.I. sensitivity obtained for 20 mm thick material is 0.5 %. This value is excellent as the radiographic film.
- (5) Within the scope of study the detectability of cracks is dependent on the incidence angle of X-rays to the cracks. It is desirably less than 9°.

Acknowledgement

The authors wish to thank Drs. S. Nomura, Y. Sasaki and T. Oku for their informative advice.

Thanks are also due to Mr. Fujisaki and the member of the Graphite Research Lab. for many experimental helps.

References

- 1) Shimokawa J. et al. : JAERI-M 6141, "Fundamental Conceptual Design of the Experimental Multi-Purpose High-Temperature Gas-Cooled Reactor" (1975)
- 2) Gomay Y., Nomura S., Fukuda K., Muraoka S. and Nakamura H. : JAERI-M 6432, "An Estimate of Low-Z Materials for the First Wall of JT-60" (1974)
- 3) Westinghouse Electric Corporation, Astro Nuclear Laboratory : WANL-TME-391, "Requirements for Unloaded Graphite Core Elements for WANL Destruction Core Test" (1973)
- 4) McClung R.W. : ORNL-3252, "Techniques for Low-Voltage Radiography" (1962)

material less than 5 mm thick, control of atmosphere and bare film exposure techniques are useful.

- (2) The absorption of radiated X-rays by air is large and it reaches to 50-60 % in case of 15 kvp of X-ray energy. At 40 kvp or more it can be neglected.
- (3) The difference in radiographic quality between two types of film, Sakura RR and Eastman M, were compared in the sensitivity and contrast. The sensitivity of Sakura RR is about 10 times higher than that of Eastman M. Image contrast depends on the thickness of material. In case of 5 and 10 mm thick material Eastman M is superior to Sakura RR, but at 20 mm there is no difference between them.
- (4) The I.Q.I. sensitivity obtained for 20 mm thick material is 0.5 %. This value is excellent as the radiographic film.
- (5) Within the scope of study the detectability of cracks is dependent on the incidence angle of X-rays to the cracks. It is desirably less than 9°.

Acknowledgement

The authors wish to thank Drs. S. Nomura, Y. Sasaki and T. Oku for their informative advice.

Thanks are also due to Mr. Fujisaki and the member of the Graphite Research Lab. for many experimental helps.

References

- 1) Shimokawa J. et al. : JAERI-M 6141, "Fundamental Conceptual Design of the Experimental Multi-Purpose High-Temperature Gas-Cooled Reactor" (1975)
- 2) Gomay Y., Nomura S., Fukuda K., Muraoka S. and Nakamura H. : JAERI-M 6432, "An Estimate of Low-Z Materials for the First Wall of JT-60" (1974)
- 3) Westinghouse Electric Corporation, Astro Nuclear Laboratory : WANL-TME-391, "Requirements for Unloaded Graphite Core Elements for WANL Destruction Core Test" (1973)
- 4) McClung R.W. : ORNL-3252, "Techniques for Low-Voltage Radiography" (1962)

- 5) McMaster R.C. : "Nondestructive Testing Handbook", The Ronald Press, New York, (1959)
- 6) JIS 3105-1968 (Japanese Industrial Standard), "Method of Radiography and Classification for Alminum Welds"

Table 1 X-ray Attenuation Coefficients of Atoms
 $(\lambda=0.098 \text{ \AA X-ray})$

Atom	Atomic number	(μ/ρ)	μ	Atom	Atomic number	(μ/ρ)	μ
H	1	0.280		Ru	44	0.90	11.1
Li	3	0.125	0.067	Rh	45	0.95	11.8
Be	4	0.131	0.24	Pd	46	0.99	11.3
B	5	0.138	0.35	Ag	47	1.05	11.0
C	6	0.142	0.33	Cd	48	1.09	9.4
N	7	0.143		In	49	1.13	8.2
O	8	0.144		Sn	50	1.17	8.5
F	9	0.146		Sb	51	1.21	8.1
Ne	10	0.148		Te	52	1.25	7.8
Na	11	0.150	0.15	I	53	1.33	6.7
Mg	12	0.152	0.26	Xe	54	1.40	
Al	13	0.156	0.42	Cs	55	1.46	2.7
Si	14	0.159	0.37	Ba	56	1.52	5.7
P	15	0.163	0.32	La	57	1.60	9.8
S	16	0.166	0.33	Ce	58	1.68	11.6
Cl	17	0.176		Pr	59	1.75	11.4
A	18	0.164		Nd	60	1.81	12.6
K	19	0.191	0.16	Sm	62	1.95	15.2
Ca	20	0.200	0.31	Eu	63	2.02	10.5
Sc	21	0.208	0.52	Gd	64	2.08	12.3
Ti	22	0.217	0.96	Tb	65	2.13	17.7
V	23	0.227	1.4	Dy	66	2.23	19.2
Cr	24	0.238	1.7	Ho	67	2.33	21
Mn	25	0.250	1.8	Er	68	2.40	11.4
Fe	26	0.265	2.1	Tm	69	2.48	23
Co	27	0.287	2.5	Yb	70	2.55	14.0
Ni	28	0.310	2.8	Lu	71	2.63	26
Cu	29	0.325	3.0	Hf	72	2.72	31
Zn	30	0.350	2.5	Ta	73	2.80	47
Ga	31	0.330	2.3	W	74	2.88	56
Ge	32	0.41	2.2	Re	75	2.95	63
As	33	0.44	2.5	Os	76	3.02	68
Se	34	0.48	2.2	Ir	77	3.09	69
Br	35	0.52		Pt	78	3.15	68
Kr	36	0.56		Au	79	3.21	62
Rb	37	0.59	0.90	Hg	80	3.31	45
Sr	38	0.61	0.6	Tl	81	3.41	41
Y	39	0.66	2.5	Pb	82	3.50	40
Zr	40	0.71	4.6	Bi	83	3.57	35
Nb	41	0.75	6.4	Th	90	3.80	48
Mo	42	0.79	7.9	U	92	3.90	73

(μ/ρ) : mass attenuation coefficient

μ : linear attenuation coefficient

Table 2 Some Properties of Graphite

Brand	Coke	Method of production	Density	Young's modulus(*)	Apparent porosity
SEG-6H	Needle	Extrusion	1.71 g/cm ³	1.51×10 ³ kg/mm ²	
SM1-24	Petroleum	Mould	1.77	0.95	19.4 %
SE2-24	Petroleum	Extrusion	1.72	1.16	
SMG	Needle	Extrusion	1.76	1.08	22.5

(*) The values are for the specimens parallel to the axis of press or extrusion

Table 3 Conditions for Crack Detectability Test

Thickness of graphite	Tube voltage	Tube current	Time of exposure
10 mm	30 kvp	2 mA	50 sec
20 mm	38	2	50
30 mm	45	2	50
40 mm	50	2	50

Film : Sakura RR

Intensifying Screen : not used

Table 4 Comparison of Image Quality Indicator Sensitivity

Thickness	Exposure	Film Density	I.Q.I. Sensitivity
20 t	40 mA-sec	Ap =2.20	Ap =0.63 %
		(Ap)=2.22	(Ap)=0.80
		(Vp)=2.25	(Vp)=0.63
	50 mA-sec	Ap =2.80	Ap =0.50
30 t	70 mA-sec	Ap =2.28	Ap =0.42
		(Ap)=2.28	(Ap)=0.42
		(Vp)=2.29	(Vp)=0.53
40 t	120 mA-sec	Ap =2.25	Ap =0.40
		(Ap)=2.22	(Ap)=0.40
		(Vp)=2.27	(Vp)=0.40

X-ray Energy : 40 kvp
 Film : Sakura RR
 Atmosphere : Air and Vacuum
 Holder : Paper

Note Ap : Air and Paper Holder
 (Ap) : Air and Paper Holder in Chamber
 (Vp) : Vac. and Paper Holder in Chamber
 (Ab) : Air and Bare Film in Chamber

Table 5 Environmental Effect on Film Density

Energy	Film Holder	Air	Chamber
20 kvp	(Ab)=1.02(Ap)	(Vp)=1.45(Ap)	(Ap)=1.08Ap
30 kvp	(Ab)=1.01(Ap)	(Vp)=1.15(Ap)	(Ap)=1.11Ap
40 kvp	(Ab)=(Ap)	(Vp)=1.01(Ap)	(Ap)=Ap
50 kvp	(Ab)=0.98(Ap)	(Vp)=(Ap)	(Ap)=Ap

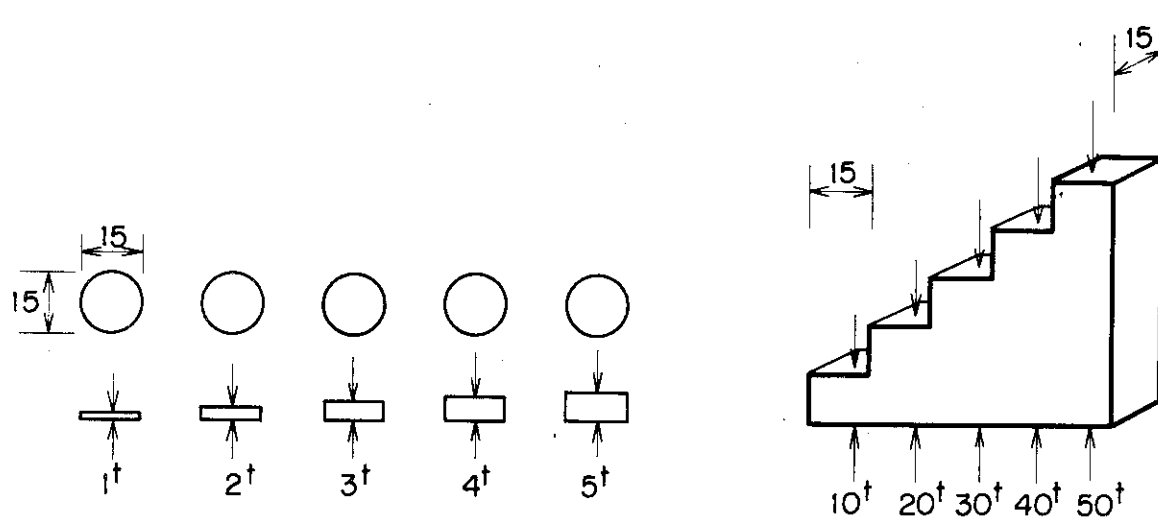


Fig. 1 Graphite step wedge

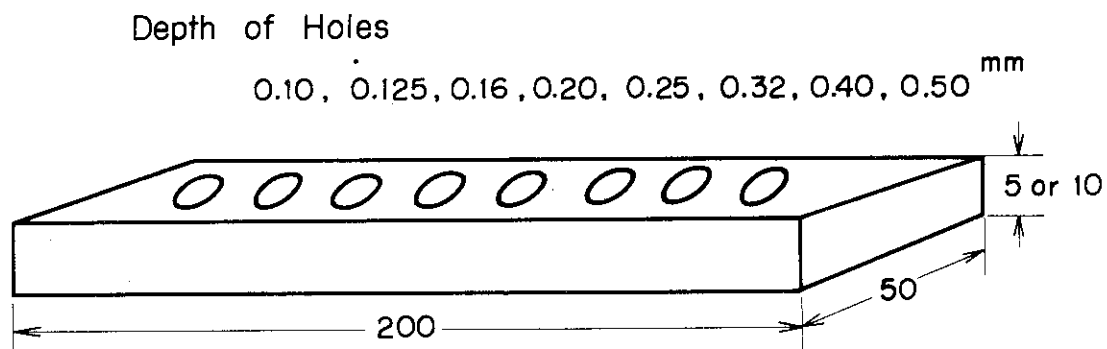


Fig. 2 Image quality indicator

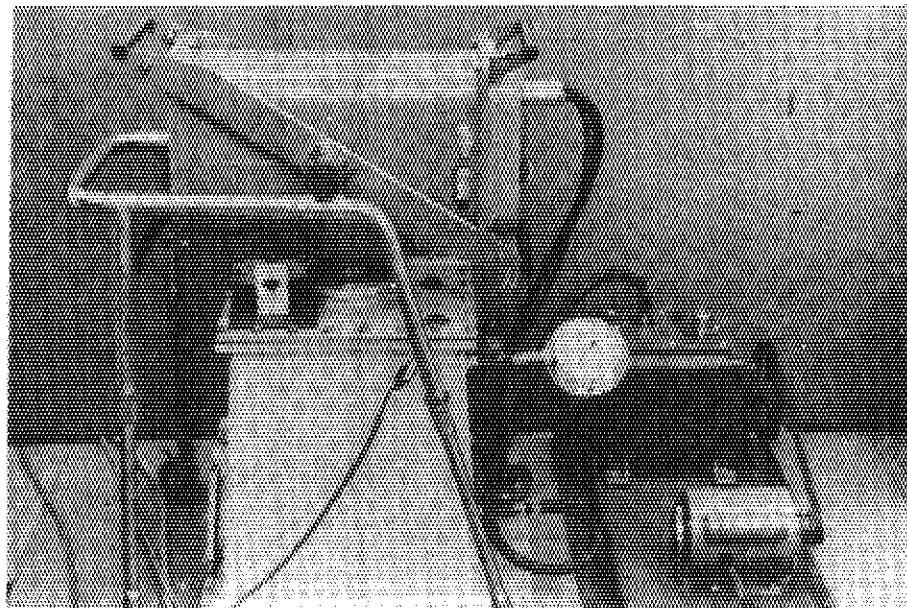


Fig. 3 Vacuum chamber

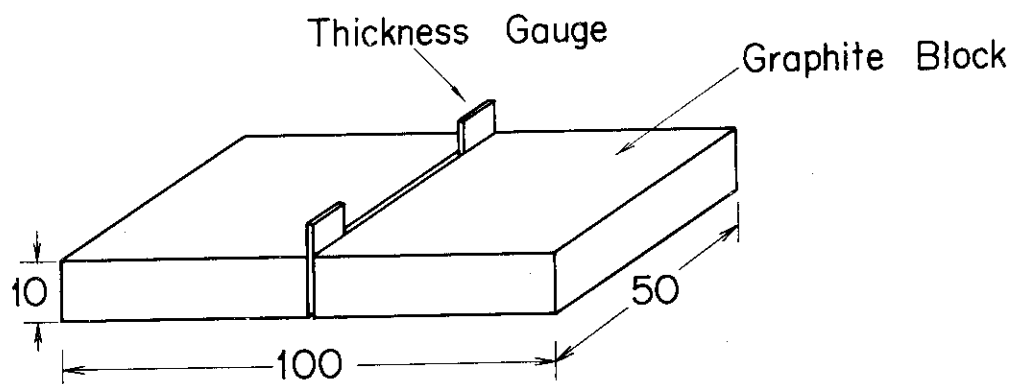


Fig. 4 Artificial crack gauge

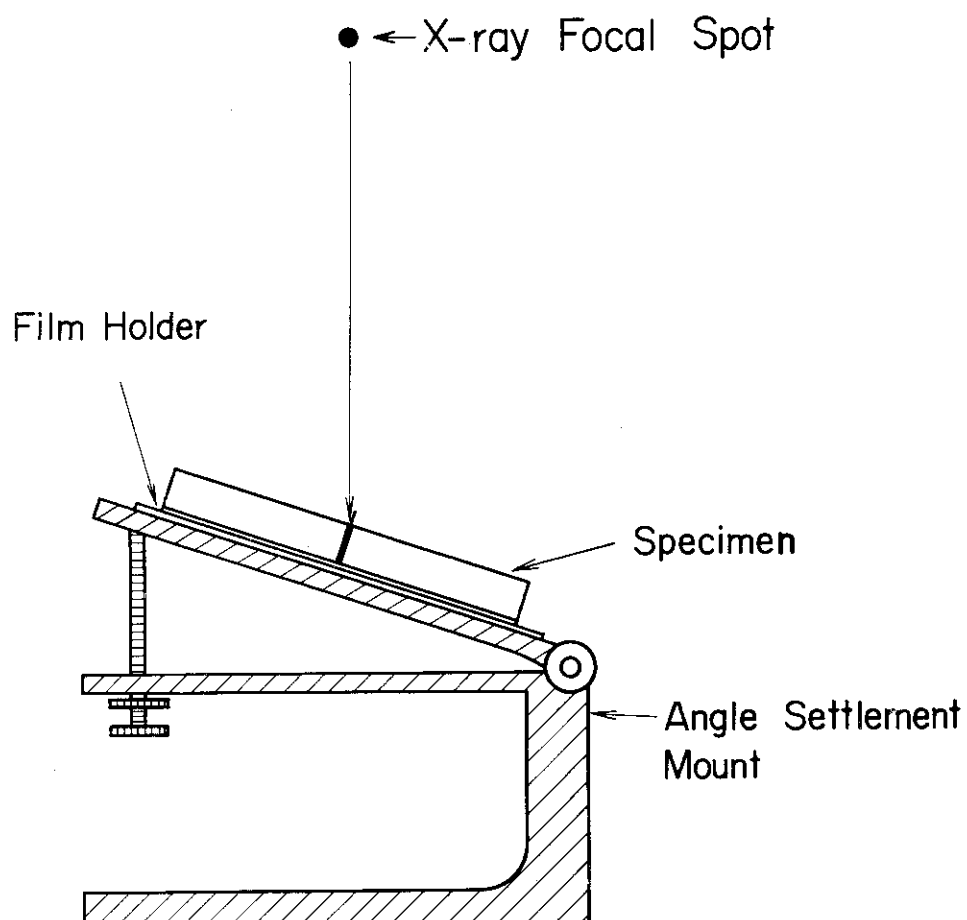


Fig. 5 Schematic figure of crack detectability test arrangement

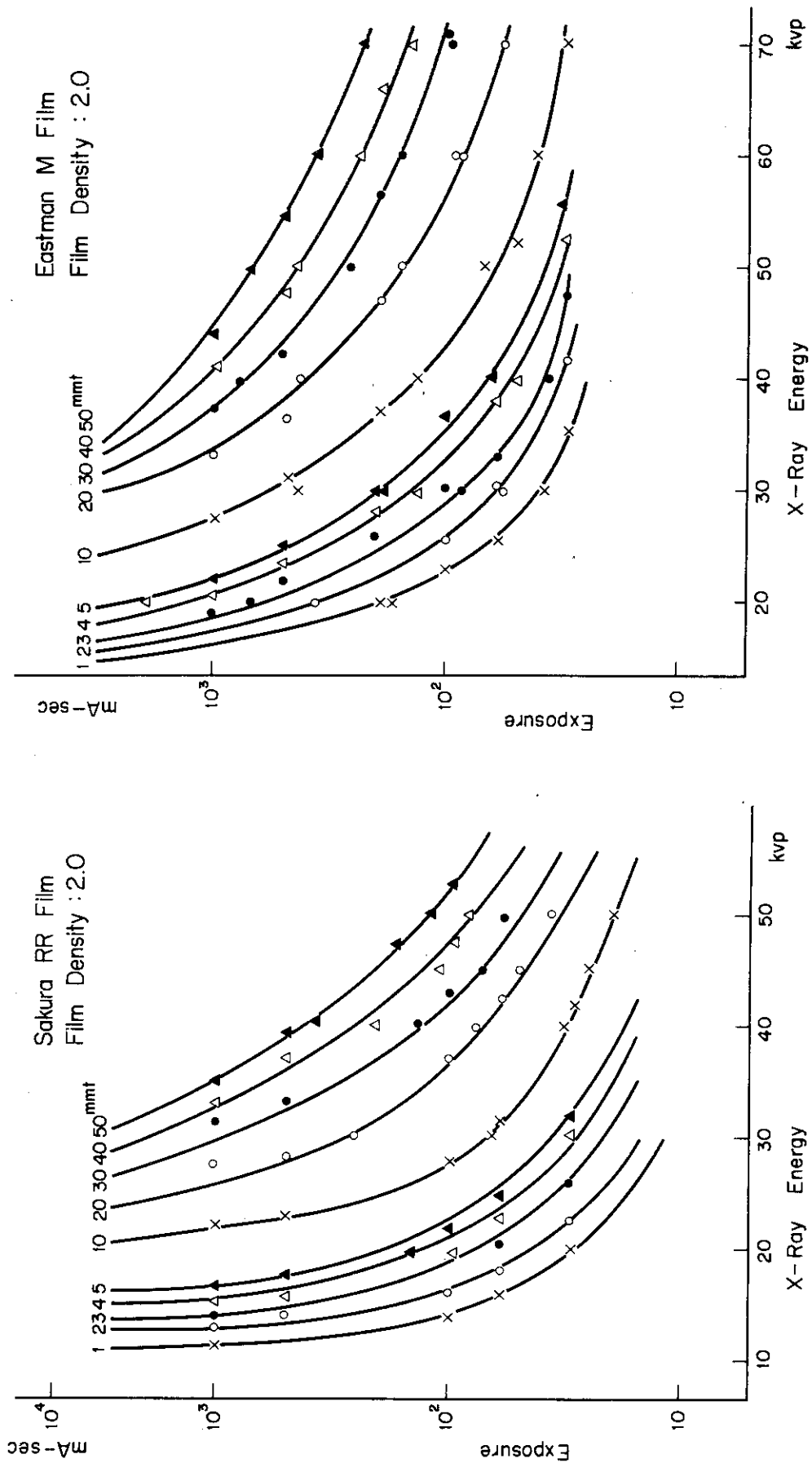


Fig. 6 Exposure chart for various thickness of graphite with air atmosphere

Fig. 7 Exposure chart for various thickness of graphite with air atmosphere

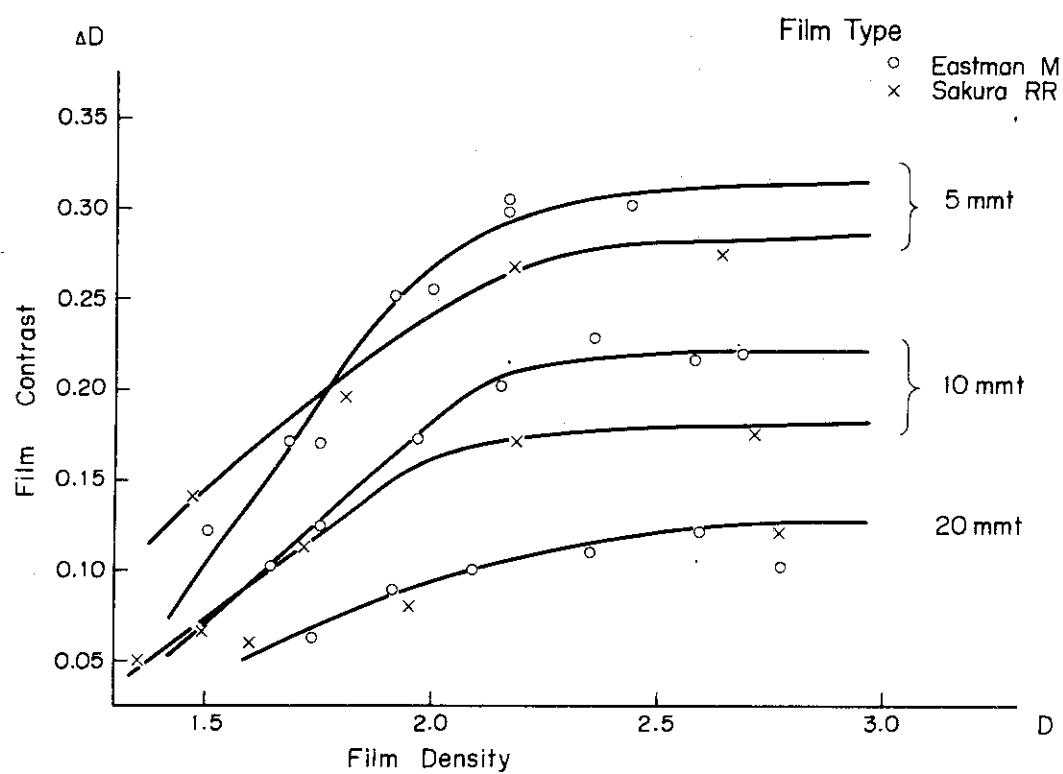


Fig. 8 Relation between film contrast and film density

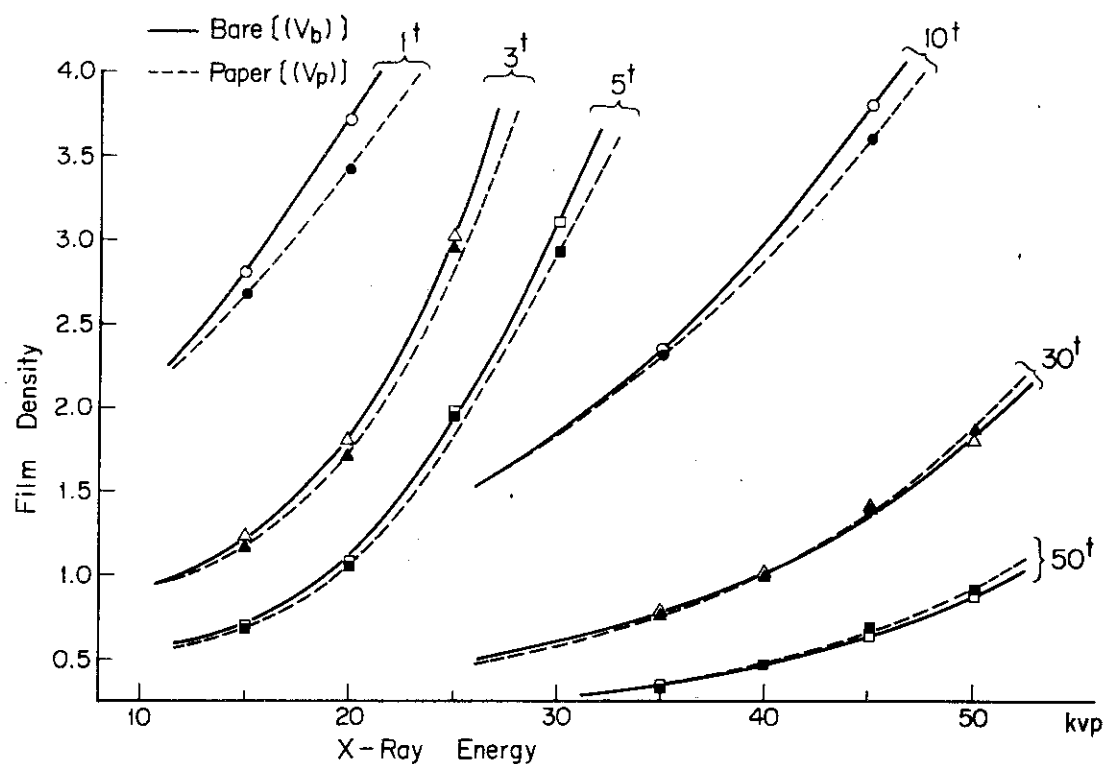


Fig. 9 Effect of film holder with vacuo

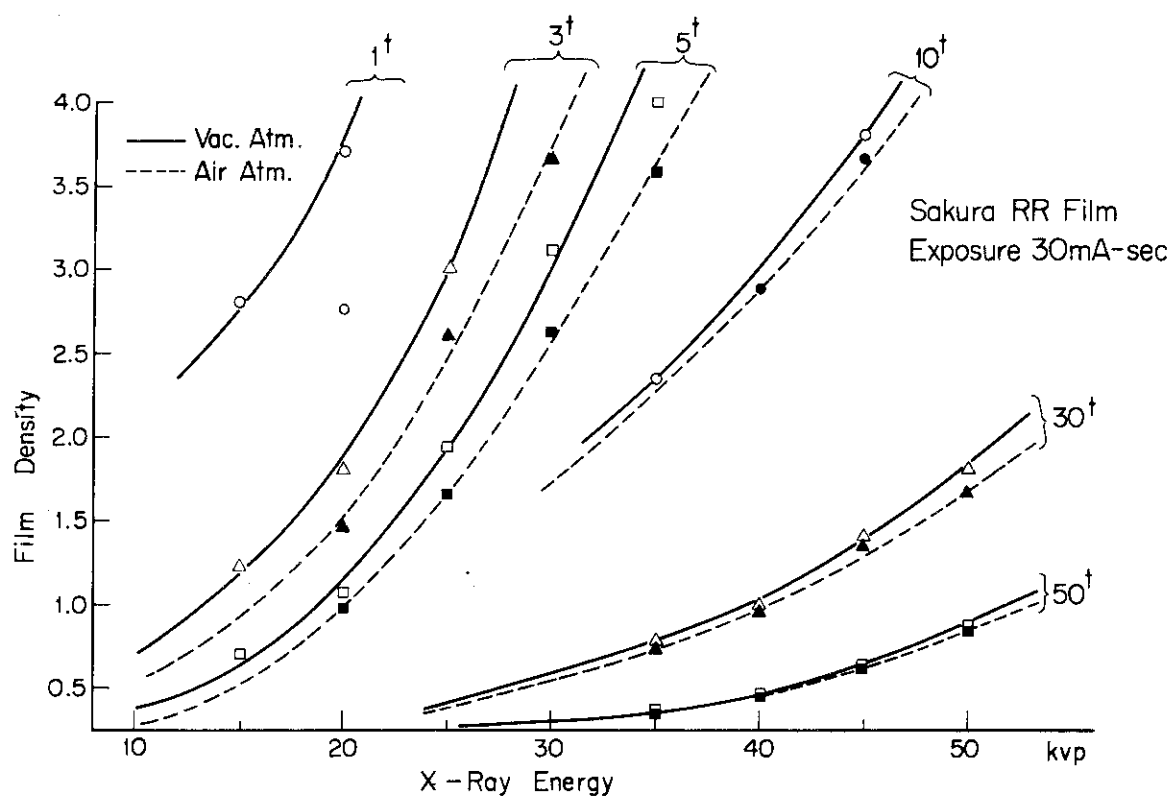


Fig. 10 Comparison of X-ray energy vs. density curves for vacuo and air atmosphere

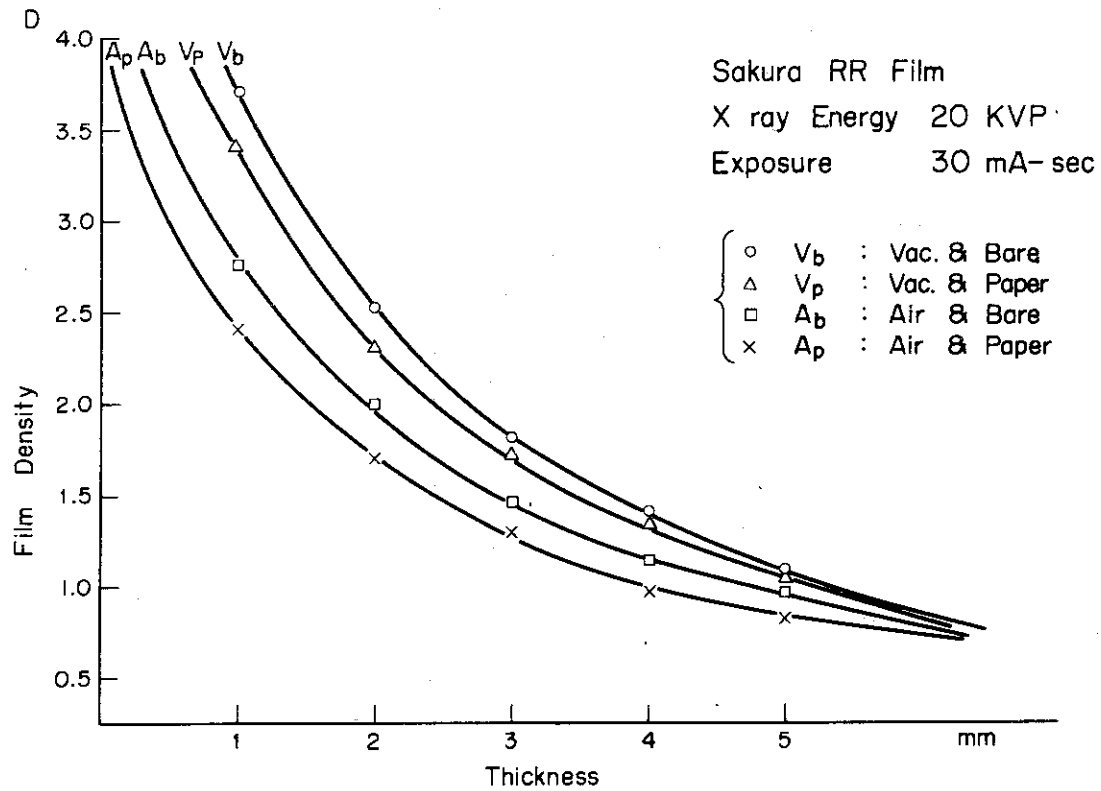


Fig. 11 Thickness vs. density curves for various conditions (1)

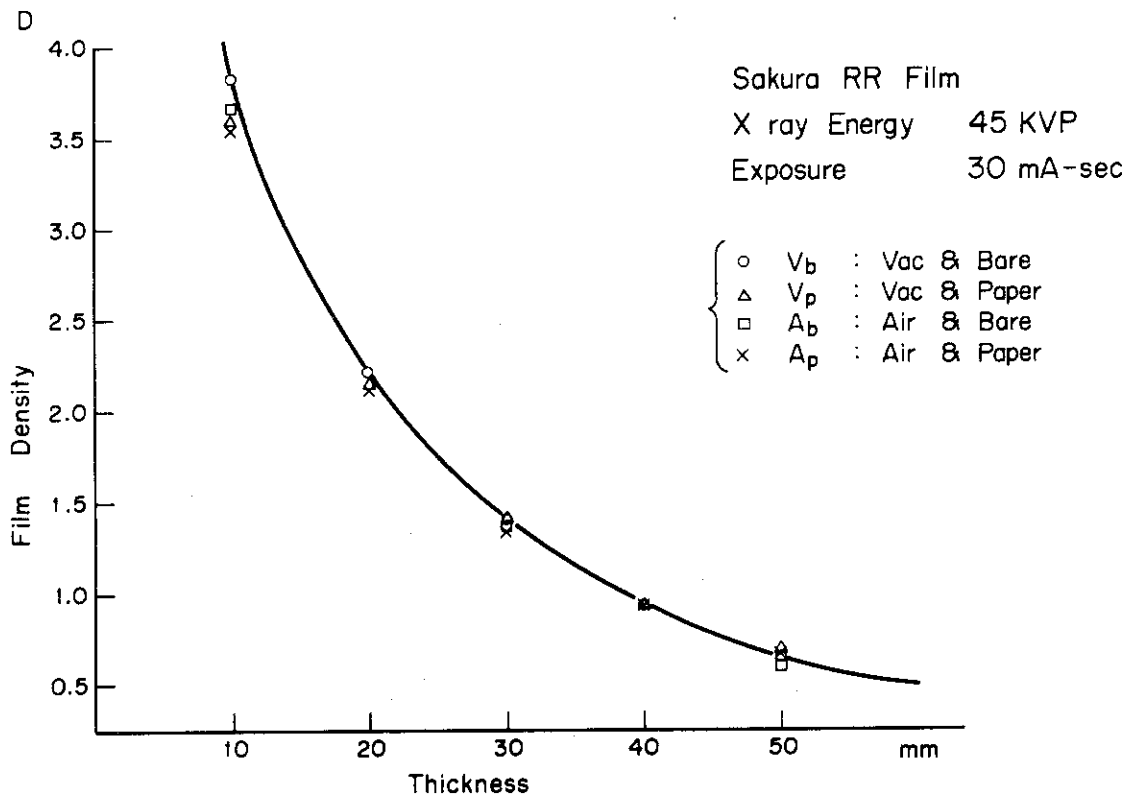


Fig. 12 Thickness vs. density curves for various conditions (2)

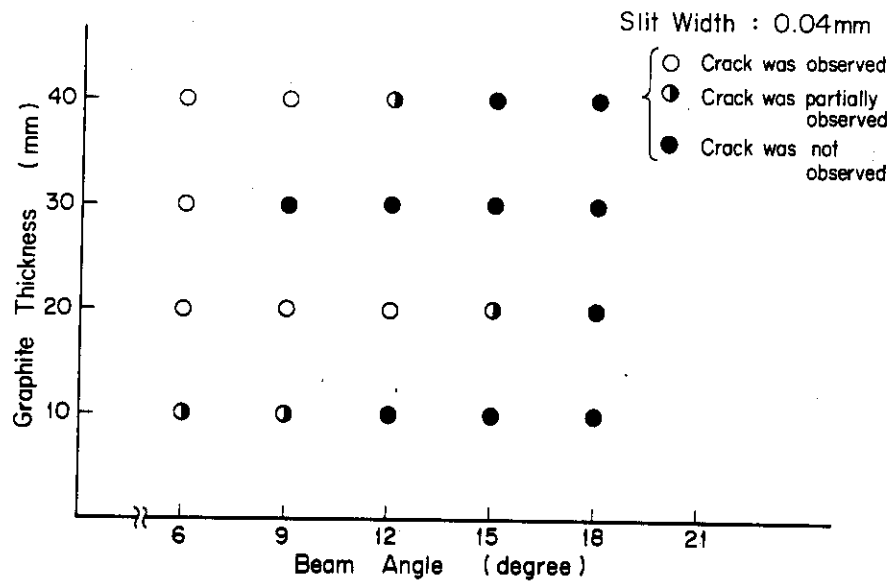


Fig. 13 Effect of inclined X-ray beam on the crack detectability limit

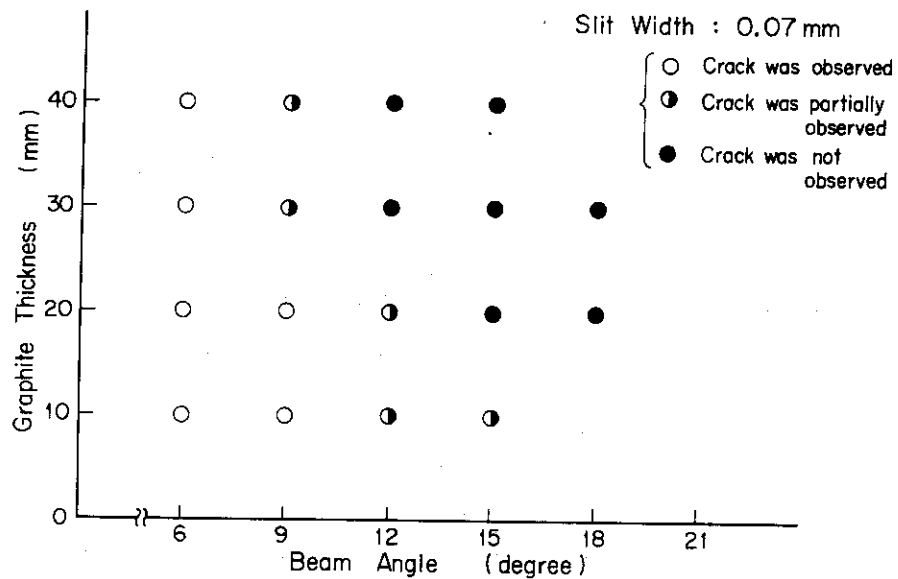


Fig. 14 Effect of inclined X-ray beam on the crack detectability limit

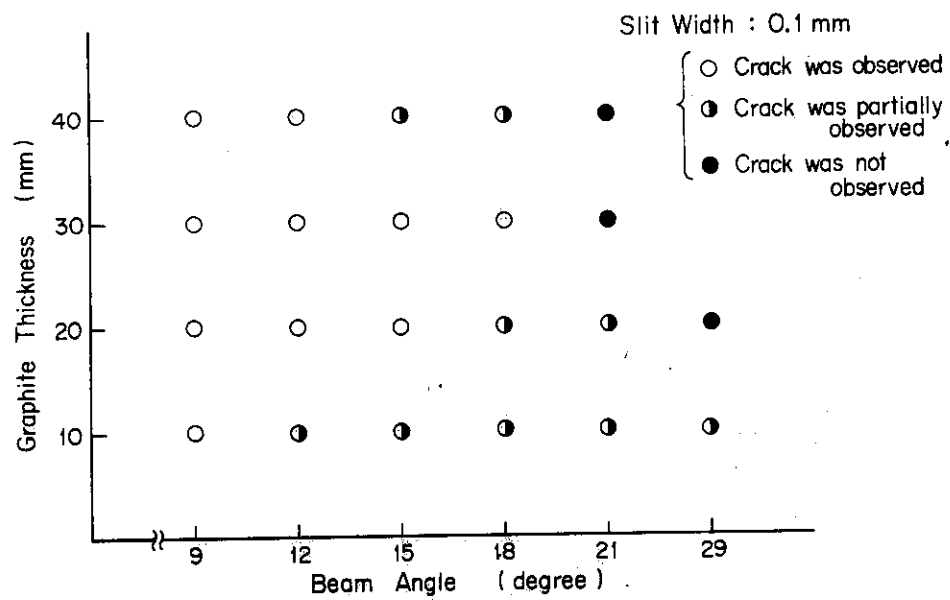


Fig. 15 Effect of inclined X-ray beam on the crack detectability limit

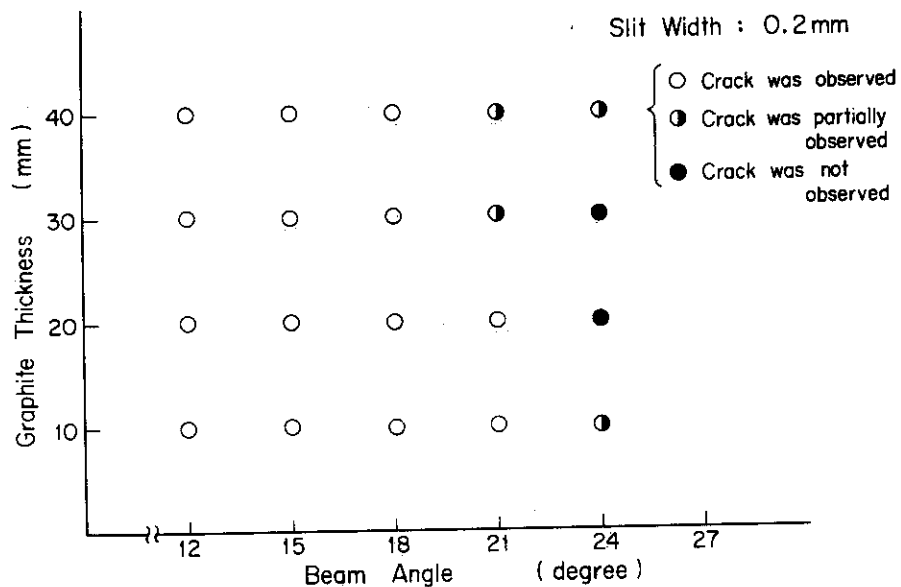


Fig. 16 Effect of inclined X-ray beam on the crack detectability limit

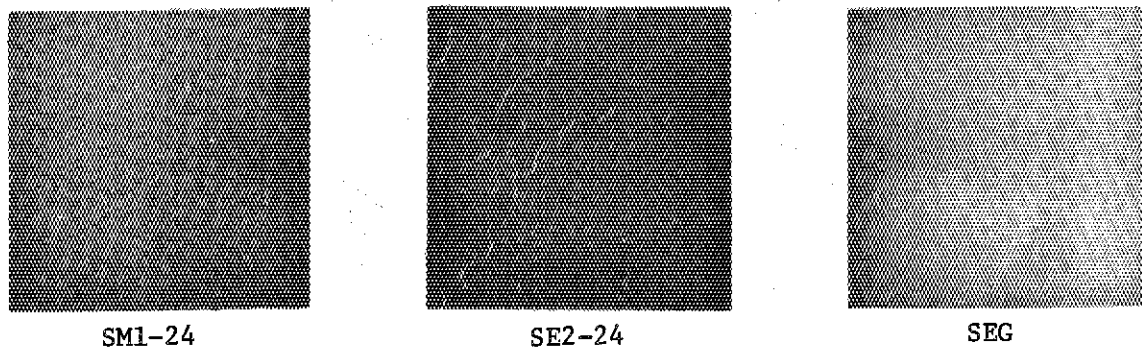


Fig. 17 X-ray radiography of three kinds of graphite

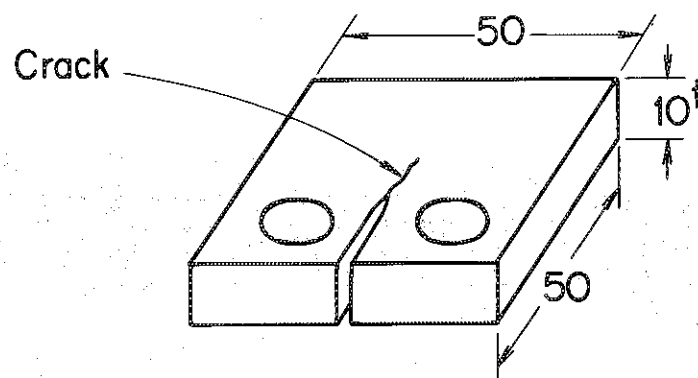


Fig. 18 Artificial crack
(Fatigue test specimen)

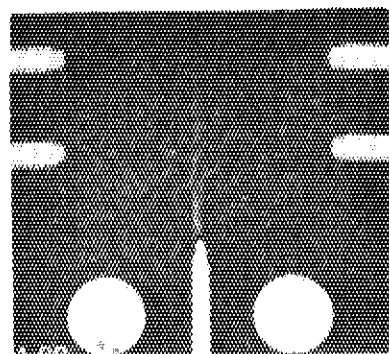


Fig. 19 X-ray radiography of the artificial crack

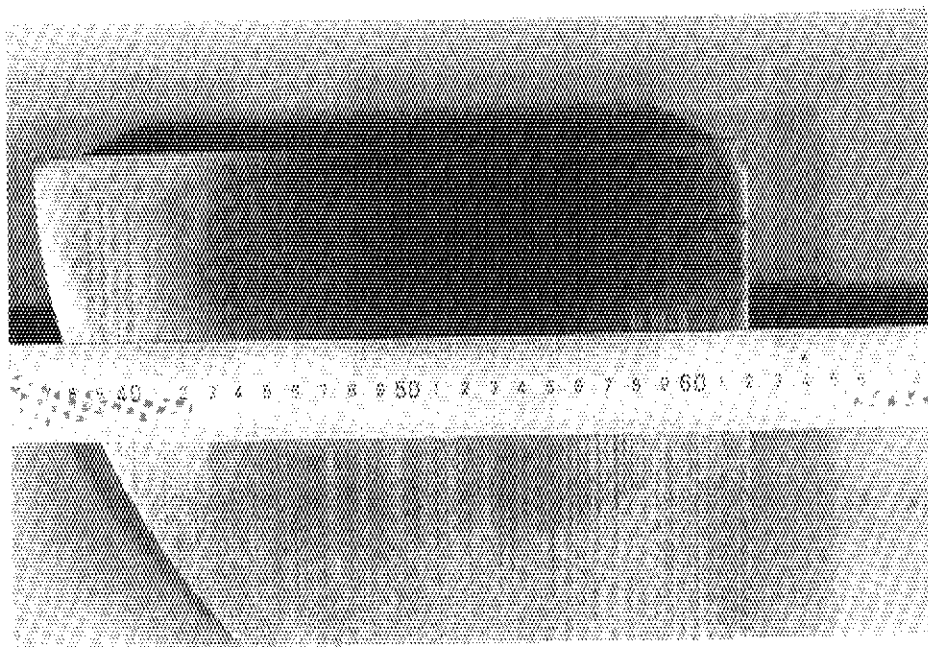


Fig. 20 External view of the cracked graphite

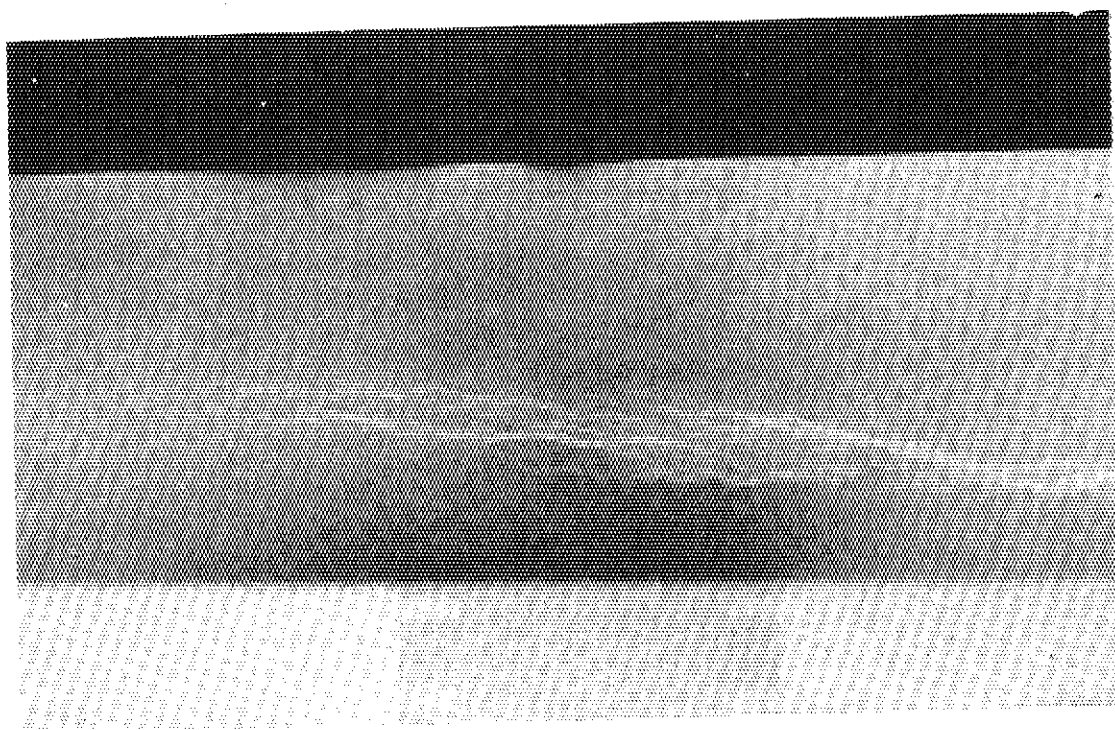


Fig. 21 X-ray radiography of the cracked graphite